USGS
science for a changing world

Evaluating Coastal Landscape Response to Sea-Level Rise in the Northeastern United States—Approach and Methods

Open-File Report 2014–1252
Version 2.0, December 2015

U.S. Department of the Interior
U.S. Geological Survey

USGS
science for a changing world

Evaluating Coastal Landscape Response to Sea-Level Rise in the Northeastern United States—Approach and Methods

By Erika E. Lentz, Sawyer R. Stippa, E. Robert Thieler, Nathaniel G. Plant, Dean B. Gesch, and Radley M. Horton

Open-File Report 2014–1252
Version 2.0, December 2015

U.S. Department of the Interior
U.S. Geological Survey

U.S. Department of the Interior
SALLY JEWELL, Secretary

U.S. Geological Survey
Suzette M. Kimball, Director

U.S. Geological Survey, Reston, Virginia
First release: 2015
Revised: December 2015 (ver. 2.0)

Suggested citation:
Lentz, E.E., Stippa, S.R., Thieler, E.R., Plant, N.G., Gesch, D.B., and Horton, R.M., 2015, Evaluating coastal landscape response to sea-level rise in the northeastern United States—Approach and methods (ver. 2.0, December 2015): U.S. Geological Survey Open-File Report 2014–1252, 27 p., http://dx.doi.org/10.3133/ofr20141252.

ISSN 2331-1258 (online)

Acknowledgments

This research was funded by the U.S. Geological Survey Coastal and Marine Geology Program, the Department of the Interior Northeast Climate Science Center, and the U.S. Army Corps of Engineers Institute for Water Resources under the Responses to Climate Change Program. Aaron Turecek of the U.S. Geological Survey assisted with data acquisition and preliminary data processing for this project. Dan Bader of Columbia University, was a contributor in the sea-level projections. We are grateful to the North Atlantic Landscape Conservation Cooperative Structured Decision Making Workshop participants and coaches for early input on decision-support needs: Andrew Milliken, Tim Jones, Kevin Kalasz, Adam Whelchel, Matt Whitbeck, Dorina Frizzera, Bill Hulslander, Brady Mattsson, Erin Rivenbark, and Krishna Pacifici. We acknowledge the World Climate Research Programme's Working Group on Coupled Modelling, which is responsible for the Coupled Model Intercomparison Project (CMIP), and we thank the climate modeling groups for producing and making available their model output. The U.S. Department of Energy Program for Climate Model Diagnosis and Intercomparison provided coordinating support and led development of software infrastructure for CMIP in partnership with the Global Organization for Earth System Science Portals. Neil Ganju of the U.S. Geological Survey and Joanna Grand of the University of Massachusetts provided helpful reviews of this report.

.

Contents

Figures

Tables

Conversion Factors

International System of Units to Inch/Pound

Multiply	By	To obtain
	Length	
meter (m)	3.281	foot (ft)
kilometer (km)	0.6214	mile (mi)
	Flow rate	
millimeter per year (mm/yr)	0.03937	inch per year (in/yr)

Datum

Except where otherwise noted in the report, vertical coordinate information is referenced to mean high water, a tidal datum that is derived from the average of all high water heights observed over the National Tidal Datum Epoch.

Horizontal coordinate information is referenced to the North American Datum of 1983 (NAD 83).

Elevation, as used in this report, refers to distance above the vertical datum.

Abbreviations

AR5	International Panel on Climate Change Fifth Assessment Report
CCSP	U.S. Climate Change Science Program
CMIP	Coupled Model Intercomparison Project
CMIP5	Coupled Model Intercomparison Project Phase 5
CRM	Coastal Relief Model [National Oceanic and Atmospheric Administration National Geophysical Data Center]
ESM	ecological systems map
GIA	glacial isostatic adjustment
GPS	Global Positioning System
IPCC	Intergovernmental Panel on Climate Change
LCAD	University of Massachusetts Landscape Conservation and Design
MHW	mean high water
NALCC	North Atlantic Landscape Conservation Cooperative
NED	National Elevation Dataset
NHD	National Hydrography Dataset
RCP	representative concentration pathway
TNC	The Nature Conservancy
USGS	U.S. Geological Survey

Evaluating Coastal Landscape Response to Sea-level Rise in the Northeastern United States—Approach and Methods

By Erika E. Lentz,[1] Sawyer R. Stippa,[1] E. Robert Thieler,[1] Nathaniel G. Plant,[1] Dean B. Gesch,[1] and Radley M. Horton[2]

Abstract

The U.S. Geological Survey is examining effects of future sea-level rise on the coastal landscape from Maine to Virginia by producing spatially explicit, probabilistic predictions using sea-level projections, vertical land movement rates (due to isostacy), elevation data, and land-cover data. Sea-level-rise scenarios used as model inputs are generated by using multiple sources of information, including Coupled Model Intercomparison Project Phase 5 models following representative concentration pathways 4.5 and 8.5 in the Intergovernmental Panel on Climate Change Fifth Assessment Report. A Bayesian network is used to develop a predictive coastal response model that integrates the sea-level, elevation, and land-cover data with assigned probabilities that account for interactions with coastal geomorphology as well as the corresponding ecological and societal systems it supports. The effects of sea-level rise are presented as (1) level of landscape submergence and (2) coastal response type characterized as either static (that is, inundation) or dynamic (that is, landform or landscape change). Results are produced at a spatial scale of 30 meters for four decades (the 2020s, 2030s, 2050s, and 2080s). The probabilistic predictions can be applied to landscape management decisions based on sea-level-rise effects as well as on assessments of the prediction uncertainty and need for improved data or fundamental understanding. This report describes the methods used to produce predictions, including information on input datasets; the modeling approach; model outputs; data-quality-control procedures; and information on how to access the data and metadata online.

Introduction

Climate change effects, such as sea-level rise and changes in coastal storm intensities (Karl and others, 2009; Bender and others, 2010; Church and others, 2013; Hartmann and others, 2013), will likely result in increased effects on coastal regions (Field and others, 2012; Moser and others, 2014; Wong and others, 2014). In particular, the combined effects of climate-driven erosion and inundation may reduce habitat area and (or) quality along sandy and (or) wetland shorelines (Craft and others, 2009; Kirwan and Megonigal, 2014) and make human infrastructure vulnerable (U.S. Army Corps of Engineers, 2013; Horton and others, 2014). These changes are expected to have a broad range of effects on natural and built environments, from affecting the breeding, nesting, and feeding behavior of

[1]U.S. Geological Survey
[2]Columbia University

threatened shorebird species such as the piping plover (Seavey and others, 2011; Gieder and others, 2014) to driving investment decisions related to the protection or abandonment of structures (McNamara and Keeler, 2013).

Assessments of future effects of sea-level rise on coastal regions vary depending on the responses that the assessments are trying to predict. The simplest assessments produce inundation scenario maps that show the flooding of existing topography to set increments of elevated sea level (Gesch, 2009; Marcy and others, 2011; Weiss and others, 2011). This type of assessment is straightforward and useful for understanding which areas are potentially vulnerable to flooding. However, coastal processes across short and long timescales (for example, storms, water-level extremes, changes to sediment flux) and other factors that drive evolution of the coast are expected to occur as sea level rises (Fitzgerald and others, 2008; Gutierrez and others, 2009), and as neither land elevation nor land-cover changes are considered, such assessments do not address the possibility of dynamic response. Spatially explicit forecasts of the interactions of oceanographic, geomorphic, and ecological processes have produced more detailed coastal evolution and vulnerability assessments in response to sea-level rise, storms, and other climate factors. However, these forecasts are accompanied by substantial and spatially variable uncertainty resulting from errors in initial elevations, limitations in understanding of the relevant processes, and uncertainty in the climate-change drivers such as sea-level-rise rates (Thieler and Hammar-Klose, 1999; Craft and others, 2009; Arkema and others, 2013), and the integration of these uncertainties with decision making related to climate change is not straightforward.

This report describes methods used to build, test, and run a sea-level-rise decision-support model that considers two coastal response types—one that is driven by inundation and one that also considers dynamic evolution of the coastal landscape. The model represents a conceptual framework aimed at supporting sound adaptive management and resource allocation strategies for the northeastern United States. The application of a structured decision-making process at the outset of this research has helped ensure that the results provided by this analysis directly address decision-making needs and are readily compatible with parallel habitat-modeling efforts. Through this modeling approach we are able to apply prediction uncertainty to identify areas where confidence levels are sufficiently high to inform decision making, and those where low confidence levels indicate improvements in data or information are needed to ensure predictions are accurate. The effects of regional sea-level-rise on the coast are predicted for four decades (the 2020s, 2030s, 2050s, and 2080s) at resolutions commensurate with those of other decision-support applications. In addition to describing the approach and the model, this report describes the input datasets and data-validation procedures, and it includes information on how to access the predictions and metadata online.

Decision-Support Requirements

The purpose of this model is to develop a geospatially explicit understanding of the probability of coastal landscape change and land loss in response to sea-level rise. This information will directly address decision-support needs elicited through a collaborative effort with the North Atlantic Landscape Conservation Cooperative (NALCC) through a structured decision-making process (Bashari and others, 2009; Ogden and Innes, 2009; Calkin and others, 2011; Martin and others, 2011; Runge and others, 2011; Marcot and others, 2012) involving regional resource managers and researchers. By requiring clear articulation of every stage of the problem to be solved, the application of a structured decision-making framework at the outset of a research project helps to ensure that the result generated will provide information necessary to tackle the problem identified rather than a result related to but not ultimately as useful to the decision-making process as another outcome might be. The coastal response information we provide will be used to inform corresponding habitat models as well as to map out

alternative management strategies to optimize conservation efforts and allocate resources for the NALCC region. As such, our study area encompasses the entire NALCC region, which extends from Maine to Virginia (fig. 1).

Several datasets are central for ensuring that our coastal response predictions meet decision-making needs. Sea-level projections are produced for time periods that either match those being used by collaborators or are common planning horizons for decision makers; vertical land movement rates, which vary throughout the region because of isostasy and other factors, are incorporated to make relative sea-level scenarios. The use of high-quality elevation data allows the projection of water-level increases across the landscape to define a general level of submergence. The land-cover base map from a corresponding habitat effects model is used to ensure that results are produced at a resolution and coverage readily usable by collaborators; land-cover information from this map is coupled with landscape submergence information to identify environment types likely to dynamically respond rather than submerge. The objectives of this assessment, therefore, are to use these datasets (land cover, relative sea-level rise, elevation), as inputs to region-wide predictions of the likelihood that a 30-meter (m) area will persist, be altered, or become submerged in the future.

Characterizations of Sea-Level Rise Effects on the Coast

We geospatially resolve the alteration and adaptability of coastal land-cover types to a range of sea-level-rise scenarios. Adjusted elevation serves as a primary variable that can be used to describe the landscape with respect to the projected sea levels. The adjusted elevation (*AE*) transforms the current [2010s] elevation (*E*), expected sea-level (*SL*), and expected geologically or tectonically controlled vertical land movement (*VLM*), as follows:

$$AE\left(\vec{x},t\right) = E\left(\vec{x}\right) - SL\left(\vec{x},t\right) + VLM\left(\vec{x},t\right) + uncertainties\,, \tag{1}$$

where

$\vec{x}$ indicates dependence on the geospatial location (that is, $\vec{x}$ = latitude and longitude) and

t indicates dependence on time.

Here, the spatial and temporal variability in sea level is presented as projected sea-level scenarios for the 2020s, 2030s, 2050s, or 2080s obtained from models, and variability in vertical land movement is presented as the calculated amount of elevation change caused by subsidence and (or) glacial isostatic adjustment based on current rates extrapolated to the times of interest. Uncertainties apply to each of the variables on the right side of equation 1.

In addition to adjusted elevation, the coastal response of the landscape is considered by identifying the likelihood that a coastal area will respond or submerge in response to sea-level scenarios. This prediction is made by combining adjusted elevation predictions with land-cover information (fig. 2). The possibilities for coastal response of the land include morphologic and ecological evolution (dynamic response) or inundation (static response) as water levels increase for six general land-cover types (table 1). There are two forms of dynamic response: one is when the initial land cover type is maintained; the other is when there is a transition to another nonsubmerged land cover type. Static response, on the other hand, occurs in areas that cannot accommodate or adapt to water-level increases and, therefore, become submerged or inundated.

Table 1. The land-cover classes falling within the six generalized land-cover categories used in this study.
[Each category assumes a similar response rate of the land-cover classes to sea-level-rise effects]

Land cover category	Land-cover classes included
Subaqueous	Bays, lakes, rivers, marine and estuarine subtidal, and deepwater
Marsh	Salt and freshwater marshes, bogs, swamps, fens, wetland forests, intertidal aquatic beds and reefs
Beach	Dune and swale/sandy beach (including bluffs), marine and estuarine intertidal unconsolidated shore
Rocky	Rocky outcrops and shores, marine and estuarine intertidal rock bottom
Forest	Forests, woodlands, grasslands, agricultural, shrublands
Developed	All National Land Cover Dataset developed classes (open space, low, medium, and high density), roads, active and abandoned railroad tracks

Coastal response predictions include prediction probabilities specific to different land cover types (table 1); including prediction probabilities allows us to address the varying degrees of complexity and understanding regarding the effects of sea-level rise across the landscape. The coastal response is determined by coupling adjusted elevation predictions with estimated probabilities of land-cover-type adaptation for each of 30 adjusted elevation and land cover scenarios (table 2). The probability of a dynamic response to adjusted elevation was specified for each combination of five discretized adjusted elevation levels (–12 to <–1, –1 to <0, 0 to 1, >1 to 5, and >5 to 10 m) and six land-cover categories (table 1). The probability of an inundation response is the dynamic response probability subtracted from 1. The resulting transition boundary table (table 2) shows these probabilities. A higher level of confidence for one outcome over the other is expressed by assigning a higher likelihood percentage to the former; where uncertainty in the two outcomes was greatest, each response type was given an equal likelihood of occurrence. The following sections describe in detail our modeling approach and how likelihoods were estimated for each coastal response scenario.

Table 2. Likelihood estimates of response for each adjusted elevation range and corresponding land-cover type.
[References are those associated with sea-level threshold rates used to inform probabilities]

Land cover type	Coastal response by adjusted elevation, in meters[1]					References
	–12 to –1	–1 to 0	0 to 1	1 to 5	5 to 10	
Subaqueous	0.90 | 0.10	0.70 | 0.30	0.50 | 0.50	0.10 | 0.90	x | x	Niederoda and others (1984); Swift and others (1985); Wright and others (1991, 1994); Orth and others (2006)
Rocky	0.05 | 0.95	0.10 | 0.90	0.50 | 0.50	0.90 | 0.10	x | x	Thieler and Hammar-Klose (1999)
Marsh	0.25 | 0.75	0.45 | 0.55	0.65 | 0.35	0.90 | 0.10	x | x	Morris and others (2002); Kirwan and others (2007); Cahoon and others (2009); Kirwan and others (2010); and Kirwan and Megonigal (2013)
Beach	0.40 | 0.60	0.85 | 0.15	0.95 | 0.05	1.00 | 0.00	1.00 | 0.00	Fitzgerald and others (2008); Cahoon and others (2009); Gutierrez and others (2009)
Forest	0.10 | 0.90	0.45 | 0.55	0.50 | 0.50	0.75 | 0.25	x | x	Clark (1986); Brinson and others (1995); Robichaud and Begin (1997); Williams and others (1999)
Developed	0.05 | 0.95	0.25 | 0.75	0.50 | 0.50	0.75 | 0.25	x | x	McNamara and Werner (2008); McNamara and others (2011); McNamara and Keeler (2013)

[1]Response is shown as dynamic | static by land cover type and adjusted elevation range. x denotes the elevation range was not included for the specified land cover type.

Modeling Approach

Bayesian networks generate robust probabilistic predictions. Assigning a probability of occurrence to a predicted outcome makes uncertainty easier for the user to assess. A number of coastal Bayesian network applications have been demonstrated to date, including wave predictions (Plant and Holland, 2011), sea-cliff erosion (Hapke and Plant, 2011), long-term shoreline change (Gutierrez and others, 2011), dune erosion (Plant and Stockdon, 2012), groundwater response to sea-level rise (Fienen

and others, 2013; Masterson and others, 2013), and overwash response (Plant and others, 2014). The conceptual model is used to guide the Bayesian network design (fig. 2) that takes the *E*, *SL*, *VLM*, and land cover type (*LC*) observational inputs and uncertainties and propagates them through the Bayesian network to provide a predicted probability for each *AE* and coastal response (*CR*) outcome.

Because we are forecasting a future state for which observations do not exist, three different equations are used to train our Bayesian network on the relationship between parameters. The inputs and outputs are allowed to take on a finite number of discrete states (fig. 3; table 3), and the equations evaluate the likelihood of the *i*th output state (and do so for all possibilities) given inputs extracted from the *j*th spatial location. The particular response might include the joint occurrence of a specific sea-level projection and a specific adjusted elevation range or prediction of coastal response type. The first equation (equation 2*A*) uses explicit relationships and input uncertainties among parameters as defined by equation 1:

$$P(AE_i) = \sum_{E,SL,VLM,LC} P(AE_i|E, SL, VLM)\, P(E|LC)\, P(SL_j)\, P(VLM_j)\, P(LC_j). \quad (2A)$$

In equation 2*A* we evaluate the *AE* outcome from discrete possibilities; the summation incorporates the input uncertainties; the first term on the right is the probabilistic relationship for equation 1 conditioned on inputs from the *j*th spatial location at a particular time; and the second term is determined by using Bayes' rule (Bayes, 1763), which captures the co-occurrence of land cover and elevation inputs:

$$P(E_i|LC_j) = P(LC_j|E_i) \times P(E_i) / P(LC_j). \quad (2B)$$

The first term on the right side of equation (2*B*)—for example, $P(LC_j|E_i)$—is the likelihood of the observation if the response (in this case, *E*) is known. That is, it is the probability of a particular *LC* type integrated over all elevation ranges. The next term—for example, $P(E_i)$—is the prior probability, or what is known about the elevation parameter before new or additional information is available, including uncertainty. The denominator is a normalization factor to account for the likelihood of the observations. The remaining (independent) terms in equation 2*A* are updated with input from our data or model sources, and are, in general, uncertain. The only exception is *LC*, which is entered as if it is known with certainty for each grid point, as uncertainty for this term is unquantified (see section entitled "Land Cover"). For *CR*, we assigned probabilities to a conditional probability table shown in table 2 on the basis of knowledge specific to each scenario of land cover (*LC*) and adjusted elevation (*AE*):

$$P(CR_i) = \sum_{AE,LC} P(CR_i|LC, AE)\, P(AE|LC)\, P(LC_j). \quad (2C)$$

$P(AE)$ is computed from 2*A* (and depends on *SL*, *VLM*, *E*, as well as *LC*), and $P(CR_i|LC, AE)$ are determined from published work or expert knowledge (see subsection entitled "Assigning coastal response type probabilities"). In our implementation, *LC* is exact (as noted previously), so the summation is only performed over the *AE* values—but using the Bayesian network allows for uncertainty in *LC* and, in general, we would integrate this uncertainty if the land cover maps included it. More information on these training methods is described in the following section and in the section entitled "Land Cover."

Table 3. Discretized bin ranges for all parameters in the Bayesian network.

Model Parameter	Discretized Bin Ranges
Projected sea-level (meters)	0 to 0.25; >0.25 to 0.5; >0.5 to 0.75; >0.75 to 2
Vertical land movement (meters)	–0.3 to <0; 0 to 0.1; >0.1 to 0.3
Elevation (meters)	–10 to <–1; –1 to <0; 0 to 1; >1 to 5; >5 to 10
Land cover[1]	Subaqueous; marsh; beach; rocky; forest; developed
Adjusted elevation (meters)	–12 to <–1; –1 to <0; 0 to 1; >1 to 5; >5 to 10
Coastal response type	Dynamic; static

[1]Detail on the land classes that fall into these general land-cover categories can be found in table 1.

The Bayesian network was constructed and trained by using Netica software (Norsys Software Corp., version 5.12, 1992–2013, http://www.netica.com/). Nodes in the Bayesian network (fig. 3) show input parameters (left) and forecasts (right); probability distributions in each box show the prior probability, or the probability of data falling within one of the specified ranges (discrete bins, table 3) given the full distribution of the regional data. Because sea level and vertical land movement bin ranges are time-step dependent, prior probabilities for these two inputs show uniform distributions; because our approach is scenario based, setting the prior probabilities in this way allows an equally likely chance of any of these projections occurring if a time step is not specified. Correlations among nodes are represented by arrows between them.

Assigning coastal response type probabilities.—Coastal response probabilities (table 2) are assigned based on sea-level-rise induced change thresholds specific to land cover categories and used to train the Bayesian network on the relationship between land cover and adjusted elevation. For each time step, the sea-level projections included in our model increase, a point that becomes important when sea-level rates in the published literature are compared with the adjusted elevation outcomes presented in the discussion that follows. Therefore, an inherent assumption in the estimates of response-type probability for the 30 scenarios is that larger time steps (2010s to 2050s or 2080s) correspond to the lowest adjusted elevation ranges (greatest levels of submergence), whereas the middle and highest elevation ranges were more likely to correspond to smaller time increments (2010s to 2020s or 2030s). Published threshold values of relative sea-level rise for marshes, beaches, and to some degree forests were incorporated by converting sea-level-rise rates to sea levels, adding estimates of vertical land movement, comparing them with the adjusted elevation estimates (equation 1), and assigning a corresponding probability of dynamic response. For other land-cover categories, documentation of threshold rates can be sparse, and the physical response to sea-level rise in many cases is straightforward; therefore, we assigned probabilities to fill the knowledge gap following research that has demonstrated the use of expert opinion as a means of quantifying a parameter or substituting outputs from highly uncertain models (for example, Bamber and Aspinall, 2013).

A number of studies have estimated threshold values for marsh adaptability to sea-level increases. Threshold sea-level-rise rates for the conversion of wetlands to subtidal environments have been modeled as a function of suspended-sediment concentrations and spring tidal ranges (Kirwan and others, 2010); predictions specific to geomorphic setting (throughout the mid-Atlantic coastal region) have included additional factors such as existing rates of relative sea level and wetland accretion, which were then evaluated for likelihood of open-water conversion at current [2010s] as well as increased sea-level-rise rates (Cahoon and others, 2009). An ensemble of five wetland adaptation models identifies threshold sea-level-rise rates for marshes globally (Kirwan and others, 2010). Along the largely microtidal northeastern coast under midrange sediment concentrations, one of these models shows

threshold sea-level rates in the 8- to 20-millimeter per year (mm/yr) range, which equates to a possible range of water-level increases of 0.4 to 0.8 m by 2050 and 0.7 to 1.4 m by 2080 (from 2010). Similarly, results from an expert panel convened as part of the U.S. Climate Change Science Program (CCSP) found that with an increase of 7 mm/yr in the sea-level-rise rate (which, when combined with the current [2010s] rate of 3 to 4 mm/yr, falls within the rate predicted by the ensemble models), approximately 80 percent of marshes would be converted to open water (Cahoon and others, 2009). These values compare well with the likelihoods estimated for this scenario; under the lowest adjusted elevation bin (–1 to –12 m), a 75-percent likelihood is estimated that the threshold condition would be reached (response would be static) and marshes would be converted to open water. An estimated 25-percent dynamic response reflects the uncertainty in this bin range, which leaves open the possibility that the variability of increases in sea-level rate, suspended-sediment concentrations, vertical accretion rate, and (or) tidal range in the area can combine in such a manner that in some instances marshes are in fact able to accommodate such water-level increases.

Higher adjusted elevations predicted by our model showed a greater chance for dynamic response over that of a static response in marsh environments; this can be interpreted as an increasing confidence in marsh adaptability at lower sea-level-rise rates. Approximately two-thirds of the marsh ensemble models show threshold sea-level rates in the 2–8-mm/yr range (Kirwin and others, 2010), which equates to a maximum of 0.4 m by 2050 and 0.6 m by 2080. Similarly, the CCSP expert panel found a nearly 50-percent likelihood that at a 2-mm/yr increase in the sea-level-rise rate (which when combined with the existing rate of 3–4 mm/yr would correlate with the above listed ensemble model range), marshes in the mid-Atlantic region would be converted to open water (Cahoon and others, 2009). To relate this finding to likelihood estimates in the coastal response model, we estimate a higher likelihood of marsh adaptability at lower elevation ranges (65 percent for adjusted elevation of 0 to 1 as opposed to 45 percent for adjusted elevation of –1 to 0 m), although these predictions reflect considerable uncertainty. Factors such as the rate of sea-level rise, the suspended-sediment concentration, and the vertical accretion rate, or some combination of these factors, will mean the difference between marsh survival and marsh conversion, but variability and uncertainty among these factors makes predicting the marsh response difficult. At the highest adjusted elevation ranges (1 to 5 m), it is very likely (90-percent probability of dynamic response) that a marsh in a given location would be able to adapt to water-level increases to remain a marsh; this agrees well with the CCSP expert panel results, in which experts estimated, at the current [2010s] sea-level-rise rate, an 11-percent likelihood of conversion to open-water conditions.

Like marshes, beaches are expected to dynamically adapt to some sea-level increases, determined in large part by the frequency of storm events, availability of sediment, and rate of sea-level rise. Where coastal sediment resources are insufficient, barrier beaches will thin, leaving them more vulnerable to overwash, segmentation through breaching, and a consequent further loss of sediment through inlet and ebb tidal delta formation (Fitzgerald and others, 2008). Because of the limited information available on threshold values for beach conversion, particularly threshold values that are regionally consistent, we draw on results from a second expert panel of 13 coastal scientists that convened—as part of the CCSP—to identify threshold sea-level-rise rates for spits, headlands, and wave-dominated barrier islands for the mid-Atlantic coast (Gutierrez and others, 2009). CCSP panel findings were provided as the likelihoods of specific outcomes at the same sea-level-rise scenarios as used for marshes (the current [2010s] rate; the current rate +2 mm/yr; the current rate +7 mm/yr). At the highest rate (current +7 mm/yr, which as shown with marshes previously, corresponds most directly to our adjusted elevation bin of –1 to –12 m), the CCSP panel estimated that threshold conditions were likely (probability 68 percent) to be reached for spits and that it was very likely (probability 90 percent)

that potential for threshold behavior would increase for wave-dominated barriers; this corresponds well with the estimated probability of about 60-percent probability (table 2) of static response for beaches, which suggests threshold exceedance is more likely than not but also reflects considerable uncertainty in the response. In all other scenarios, the CCSP panel was virtually certain (99 percent) that morphological changes caused by erosion, overwash, and inlet formation would be found on spits and wave-dominated barriers and that headlands would experience increased erosion; comparatively, we see an increasing likelihood of dynamic response estimated in the model (85 percent; 95 percent; and 100 percent corresponding to bin elevation increases), suggesting the highest areas are the least likely to transition to another land class category and that lower areas are more likely to transition. Although our coastal response model is only based on the likelihood of vertical change per cell and does not include an element of landward translation, we see that translation as driven by these processes for beaches is implied in the increasing dynamic certainty observed in the predictions of coastal response type.

Threshold values for the modeled land-cover conversion of the remaining types have not been explicitly estimated by the existing literature; therefore, the approach presented here demonstrates how a probabilistic model can be applied to constrain and parse prediction uncertainty. Forests are on the whole expected to have a slow adaptability response to sea-level increases; published literature documents that it is the coupling of sea-level increases with additional stressors such as episodic events—fire, wind from severe storms, land-use change—that damage the mature canopy (Clark, 1986; Brinson and others, 1995; Robichaud and Begin, 1997; Kirwin and others, 2007) and more gradual groundwater inundation that limits recruitment failure and drives forest erosion, flooding, or conversion into marsh (Robichaud and Begin, 1997; Williams and others, 1999; Kirwin and others, 2007). The probabilities estimated for the coastal response type incorporated in the model reflects this understanding and the accompanying uncertainty; end-member adjusted elevations show a strong likelihood (90 percent) of forest submergence (static response) in the range of –12 to –1 m, whereas there is a some likelihood or at least potential for forest adaptation (dynamic response) in the 1- to 5-m elevation range (75 percent). Middle-range adjusted elevations (–1 to 0 and 0 to 1 m) show response-type predictions of near total uncertainty (about 50 percent) where unknowns, such as the sea-level-rise rate and location specific stressors, make more definitive predictions impossible at this elevation range.

The remaining land-cover categories have response types that are straightforward to forecast on the basis of the limited mobility of the substrates from which they are composed or of their built environments. Rocky categories by definition are composed of hard material and therefore unable to adapt to sea-level increases; we see near certain submergence predictions in the two lower elevation ranges, with near certain dynamic response (no submergence, therefore no change in land-cover class) in the elevation ranges above mean high water (MHW; table 1). Developed areas are by definition composed of 50- to 100-percent impermeable material (Fry and others, 2011) and, in addition to flooding from the shore, are vulnerable to groundwater inundation from rising water tables (Rotzoll and Fletcher, 2012). Further uncertainties include the likelihood, spatial extent, and frequency of human modifications, such as beach replenishment, which depend heavily on socioeconomic factors and the rate of coastal change in response to storms and sea-level rise in a given area (McNamara and others, 2011). In elevations that fall below the adjusted mean sea level, our predictions are near certain of submergence or flooding (probability 95 and 75 percent). At elevations above the adjusted MHW (or adjusted elevation), uncertainty increases, reflecting the possibility that human modifications to vulnerable areas at very low elevations can prompt or permit adaptation or mitigation, depending upon the rate at which sea level rises. In the 0- to 1-m adjusted elevation range, a largely uncertain response is estimated (50 percent) because of an unknown human-response element, which is an important factor in these locales. The highest adjusted elevation level shows a moderate likelihood of dynamic response

(75 percent). This estimate reflects the knowledge that at sufficient elevations, the area is not at risk of flooding, has the potential for human response and (or) coastal modifications that can be employed more effectively than at lower elevations, can adapt under a slower sea-level-rise scenario, or some combination thereof.

The coastal response type estimates for the subaqueous category indicate the adaptability of the submerged environment type and (or) substrate to sea-level scenarios. In deepwater areas (–12 to –1 m), there is high confidence that water-level increases were likely to result in minimal overall change to the environment type or substrate (90-percent dynamic) (Wright and others, 1994). At moderate elevations, shallow subaqueous/subaerial environments are more likely to be sensitive to water-level increases caused by influences from waves, tides, sediment transport and resuspension, and sunlight attenuation (among other influences) than deeper environments (Niederoda and others, 1984; Swift and others, 1985; Wright and others, 1991; Orth and others, 2006). Therefore a decreasing dynamic response likelihood (70 percent; 50 percent; and 10 percent) was estimated at elevations just below (–1 to 0 m), at (0 to 1 m), or slightly above (1 to 5 m) the adjusted MHW. These areas were read as increasingly unable to adapt and therefore estimated as likely to become submerged.

Model Inputs

The descriptions of the input datasets used in the Bayesian network explain both the source of the data and how they were treated to fit the Bayesian network model. This treatment includes assigning continuous variables to discrete bins (table 3) whose units are elevation measures in meters (*E*, *SL*, *VLM*, *AE*). Each of the variables includes an uncertainty estimate that reflects the uncertainties in measurement (*E, VLM*), analysis (*SL*, *VLM*, *CR*), and the propagation of these uncertainties (*AE*, *CR*).

Sea-Level Projections

Global sea-level projections generated by using representative concentration pathways (RCPs) scenarios for the 2014 International Panel on Climate Change (IPCC) Fifth Assessment Report (AR5) are used as model inputs. Projections use RCP scenarios 4.5 and 8.5. Three components comprise sea-level projections: those related to oceans (both local ocean height and global thermal expansion); icemelt; and global land water storage. Of these components, local ocean height and global thermal expansion estimates are generated from 24 Coupled Model Intercomparison Project Phase 5 (CMIP5) models (Taylor and others, 2012), which provided simulations to AR5; local ocean heights are estimated by regridding global estimates to a 1- by 1-degree grid. Icemelt from the Greenland Ice Sheet and the two Antarctic Ice Sheets was estimated on the basis of the expert elicitation of Bamber and Aspinall (2013); the contributions of the glaciers and ice caps was estimated on the basis of Marzion and others (2012) and Radić and others (2013). For the ice-loss terms, no local fingerprints associated with gravitational, isostatic, and rotational effects resulting from ice-mass loss were included. Components of land water storage were incorporated into the model on the basis of Church and others (2013). For each of these three components of sea-level change, set percentiles (10th, 25th–75th, and 90th) of the distribution were estimated, and these percentiles were used to represent sea-level uncertainty. The sum of all components at each percentile is assumed to give the aggregate sea-level-rise projection. This method does not take into account potential correlation among components. For these reasons and others, these sea-level-rise projections should be thought of as scenarios, not fully probabilistic predictions. Decadal projections for the 2020s, 2030s, 2050s, and 2080s were generated by averaging across 10-year intervals and subtracting average values for 2000 to 2004. Time can be inferred from the

sea-level bins in the Bayesian network; the extents of the four bin ranges correspond to the high (75th to 90th) water-level projections for a specific time step (figs. 3, 4; table 3).

Vertical Land Movement Estimates

Vertical land movement rates (caused largely by glacial subsidence and rebound) are incorporated with the sea-level projections by using vertical velocities measured from Global Positioning System (GPS) data (Sella and others, 2007) and estimated by using tide station records (Zervas and others, 2013), as shown in figure 5. Vertical motion was determined by using interpolated grids generated from a dataset of 362 continuously recording GPS devices throughout North America that were recently processed to account for glacial isostatic adjustment (GIA). Additional estimates generated by using a methodology that extracts oceanographic effects from relative sea-level rates to determine local vertical land movement rates from records of long-range tide stations were incorporated at 69 coastal locations (Zervas and others, 2013). Uncertainties provided for each dataset (specific to each station at 1 sigma) were averaged to provide an overall vertical land movement 1 sigma uncertainty estimate of 1.6 mm/yr. For integration with other inputs, vertical land movement rates were converted to meters; rates were multiplied by the time elapsed since 2010 to keep time increments decadal. Bin ranges correspond with moderate (0 to 0.1 m) and more extreme levels (–0.3 to <0; >0.1 to 0.3 m) of GIA as a product of the estimated rate and time. Measurement uncertainty for vertical land movement parameters is also reflected in bin divisions (fig. 3; table 3) in that bin boundary values are not more resolved than the estimated dataset uncertainty.

Elevation

Topographic data were acquired from the National Elevation Dataset (NED) (Gesch, 2007). Complete regional coverage is available at 1/3 arc-second (about 9-m cells), whereas partial coverage at higher resolution (1/9 arc-second; about 3-m cells) is also available. The 1/3-arc-second data come from a combination of topographic maps, aerial photos, and lidar, whereas the high-resolution data in the 1/9-arc-second NED are from bare-earth lidar datasets (Gesch, 2007). Both are referenced to the North American Vertical Datum of 1988. Lidar data in the NED were collected by a variety of Federal, State, and local partners between 2001 and 2011.

Bathymetric data were obtained from the National Oceanic and Atmospheric Administration National Geophysical Data Center's Coastal Relief Model (CRM). These data are available at a 3-arc-second (about 90-meter) resolution and are produced by using hydrographic soundings data from the National Ocean Service and a number of academic institutions (National Oceanic and Atmospheric Administration, 2014). CRM data are used where NED data are unavailable for submerged areas such as bays, estuaries, and open ocean coasts.

We used the highest resolution elevation data available to discern elevation changes along low-lying coastal topography at increments small enough to correspond with 21st-century sea-level-rise rates between 2010 (our start date) and 2080. This means that the 1/9-arc-second data from the NED are used where available, supplemented by the 1/3-arc-second NED data where gaps in the 1/9 coverage exist, and CRM data are used where NED data are unavailable (fig. 6). Following Gesch (2009), uncertainties (root mean square error) for the 1/9- and 1/3-arc-second NED data are estimated at 0.42 m and 1.25 m. The topographic datasets were converted from the North American Vertical Datum of 1988 to MHW by using VDatum conversion grids at 6-arc-second resolution as supplied by VDatum (National Ocean Service, 2012). Vertical datum shifts to MHW were propagated landward through Euclidean allocation, which smooths vertical ledges at edges of VDatum zones. Coastal Relief Model (CRM) DEM data were not vertically referenced to MHW, as a significant portion of the CRM DEM (about 80 percent)

remained within the same elevation range when applying MHW conversion (because the model uses elevation ranges instead of discrete values). Furthermore, CRM vertical datum conversion to MHW did not cover the full extent of the study area (about 9 percent loss) and an additional percentage (about 10 percent) of the MHW conversion exceeded the vertical accuracy (±1.0 m). Therefore the CRM remain primarily referenced to MLW with a vertical accuracy of ±1.0 m (National Ocean Service, 2012).

In addition to providing essential input information, the elevation data were used to define the extent of the coastal zone for the Bayesian network. Elevation data extend seaward to –10 m (referenced to mean low water), which generally corresponds to the base of the open Atlantic Ocean shoreface in the study area, along and across which the exchange of sediment between subaerial and subaqueous environments occurs (Swift and others, 1985; Wright and others, 1994). The landward extent of the data is generally bounded by the 5-m elevation contour (above MHW), though in some cases land elevations above 5 m have been included to provide continuous coverage of features with a high likelihood of dynamic response. Bluffs, dunes, and sand beach areas (or areas coded as "beach" as described in the land-cover section that follows) and within an elevation range of 5 to 10 m were therefore included in addition to the land areas at 5 m or below. Bin ranges (table 3) encompass these greater elevation ranges, where effects to the ecosystem and (or) geomorphology are less likely, and more moderate ranges (–1 to 0 and 0 to 1 m), where sea-level projections are likely to have greatest chance of exceeding sea-level thresholds for various environment types and therefore are important to classify for decision support.

Land Cover

Land-cover information was obtained from the Ecological Systems Map (ESM) Plus (ESMplus) dataset provided by the University of Massachusetts Landscape Conservation and Design (LCAD) model (http://www.umass.edu/landeco/research/dsl/dsl.html). ESMplus uses The Nature Conservancy (TNC) Northeast Terrestrial Wildlife Habitat Classification System of 2010 (http://rcngrants.org/content/creation-regional-habitat-cover-maps-application-northeast-terrestrial-habitat) as a base. Changes or additions to the TNC base map were incorporated from additional datasets and information deemed important to the LCAD model. LCAD documents the following changes made to ESM to generate ESMplus:

- Road and train track misalignment issues were corrected (source: Open Street Map roads, at http://www.openstreetmap.org/#map=5/51.509/-7.778);
- Estuarine and marine classes were used to replace ESM estuarine classes (source: National Wetlands Inventory, 2013 at http://www.fws.gov/Wetlands/NWI/index.html);
- Five development and two agricultural classes were used to replace ESM single-developed and agriculture classes by replacing those cells in the ESM (source: National Land Cover Dataset, 2011 at http://www.mrlc.gov/nlcd2011.php);
- High-resolution streams and road-stream crossings were empirically derived (sources: National Hydrography Dataset (NHD) at http://nhd.usgs.gov/; high-resolution vector streams; Open Street Map vector roads data at http://www.openstreetmap.org/#map=5/51.509/-7.778); and
- Dam data originated from TNC's Northeast Aquatic Connectivity project and included data compiled from the U.S. Army Corps of Engineers National Inventory of Dams (http://geo.usace.army.mil/pgis/f?p=397:12:) and individual States. These data were modified through alignment with the NHD 1:24,000 high-resolution streams by using a combination of the reach code, distance to stream, and visual inspection.

Uncertainty is a known and unquantified element of the land-cover dataset. Error, for which more robust calculation is in progress (Jin and others, 2013), is present in some of the base maps, and the integration of additional datasets listed with the base layers to create ESMplus will compound this error. Because little information is available on the land-cover-classification error, we have not assigned an uncertainty value to the dataset at this time. This potentially limits our model because of misclassification of parts of the landscape that could affect prediction outcomes. Despite this limitation, we do not anticipate that land-cover uncertainty, when available, will grossly alter our predictions. The Bayesian network is designed in such a way that the important relationships among the input parameters are captured and should be preserved even with the addition of land-cover uncertainty. This is particularly true because of the generalization of the land-cover information for modeling purposes. As error calculations and analyses are completed for this dataset, an uncertainty value can easily be incorporated in the Bayesian network and predictions correspondingly updated.

For integration with the Bayesian network model, land-cover classes from ESMplus were assigned to generalized land-cover categories. Of the 197 land-cover classes in ESMplus, land-cover categories with distinctive responses to sea-level-rise effects—morphologic, ecologic, or caused by human influence—were established to assess the likelihood of land loss. Each category therefore anticipates a similar response and rate of response to sea-level-rise effects among the land-cover classes within them. The six categories and general summaries of the land-cover types in them are provided in table 2; their distribution and a comparison of them with the original ESMplus categories is shown in figure 7. To ensure seamless integration with habitat models being concurrently developed, the land-cover data at 30-meter resolution were converted to point values and used to extract values from sea-level, vertical land movement, and elevation layers. The Bayesian network was trained on the relationship between land cover and elevation by using the colocated input information from both datasets at each point; the relationship established between these two inputs allows us to observe how elevation constrains the distribution of land-cover types throughout the region and to parse uncertainties in both adjusted elevation and coastal response according to land cover.

Model Predictions

Similarly to input datasets, the predicted variables (*AE* and *CR*) were discretized into five finite elevation ranges (adjusted elevation) and two outcome scenarios (coastal response). An example of the predicted outputs is shown in figure 8. Additional detail on the data outputs, including processing steps to produce predictions and their geospatial displays, can be found in the metadata for this report (Lentz and others, 2015; http://dx.doi.org/10.5066/F73J3B0B).

Adjusted Elevation

Predictions of adjusted elevations with respect to projected MHW levels were discretized into five possible ranges: –12 to <–1 m; –1 to <0 m; 0 to 1 m; >1 to 5 m; and >5 to 10 m. Bin ranges encapsulate both end members (submerged or at elevations that exceed sea level projections and remain dry) as well as moderate elevation ranges where a variety of sea-level-rise effects are more likely to be observed. Monte Carlo simulations are run by using the 60 unique scenarios determined by equation 1—because of discretization of the input data with four sea-level bins, three vertical land movement bins, and five elevation bins—which in turn train the Bayesian network to make region-wide forecasts of adjusted elevation in lieu of observational data. Because there are a finite number of unique scenarios, probabilities assigned by the Bayesian network inherently incorporate correlations among inputs, in that scenarios seen most frequently are predicted with greater confidence than are other, less

common scenarios. This category has two outputs: the first shows the most probable elevation range for a given time step (adjusted elevation); the second shows the probability that an observation at that range will be observed. Adjusted elevation results (fig. 8*B*) show only the prediction that is most likely to occur (the bin that has the highest probability associated with it). Adjusted elevation probability rasters (fig. 8*C*) indicate the level of confidence in the adjusted elevation prediction; higher probabilities indicate greater certainty, whereas lower probabilities indicate greater uncertainty. Because these predictions are generated on the basis of data values and a fixed relationship among them (equation 1), uncertainty in adjusted elevation predictions is attributable to projected sea levels and data quality rather than limited knowledge or understanding of response. By identifying where data quality is limited, such information can be used by decision makers to determine where future data-acquisition efforts might be focused. Sea-level projections also reflect increasing uncertainty through time, which can be similarly used to establish planning horizons for decision support.

Coastal Response Type Probability

Predictions of coastal response type (equation 2*B*) are determined by coupling adjusted elevation predictions with estimated probabilities of land-cover-type survival for each of the 30 coastal response scenarios (table 1). The predictions include the underlying uncertainty associated with the coastal response expert knowledge (table 2), as well as the propagated uncertainty in the adjusted elevation. An example of a coastal response prediction result is shown in figure 8*D*. Dark colors show areas where the predicted coastal response has highest confidence; beige areas show areas where uncertainty is greatest. Unlike the adjusted elevation, uncertainty in this dataset can either be a result of data quality and sea-level projections, or, as explained earlier, an indication of limited knowledge or understanding about the processes and (or) response of a certain land cover to sea-level rise. In addition to adjusted elevation, therefore, the uncertainty in these predictions can be used to highlight where knowledge of the physical process or response of a certain environment type may be limited and, consequently, where and in which environment types future efforts or research needs may be greatest.

Application of Predictions to Decision Support

As defined in the structured decision-making process, the optimization of resources and conservation efforts for the NALCC is a two-part decision problem requiring (1) the identification of possible locations of current [2010s] and future land area that provide important habitat or ecosystems services and (2) an understanding of how these areas may fare under a variety of sea-level rise scenarios. Adjusted elevation and coastal response predictions address the latter part of this problem by providing decision makers critical information in terms of the future adaptability and corresponding uncertainty of the landscape to such scenarios. Understanding not only where land is likely to submerge but also the likelihood that the landscape can cope with that change at the output resolution provided can help decision makers to identify areas of resiliency and areas that may provide for transition and (or) buffering from sea-level-rise effects on a variety of spatial scales. Areas of considerable response uncertainty can also help to guide decision-making efforts in determining where data-collection efforts and research to improve knowledge on processes and (or) response might be focused, or, alternatively, where limited resources might be better used elsewhere. Coupled with corresponding habitat and ecosystem modeling efforts, such information can be used to address the first part of this problem, identifying locations of important habitat or ecosystems services, to locate prime areas for conservation. With this information, decision makers can evaluate where land may need to be acquired or managed differently, now or in the future, to ensure sound implementation of efforts and resources throughout the region.

Dataset Access and Assessment

Three grids showing adjusted elevation ranges (fig. 8*B*), their associated probabilities (PAE; fig. 8*C*), and probability estimates of coastal response type (fig. 8*D*) have been produced in ArcGIS raster format for each of the four prediction decades (the 2020s, 2030s, 2050s, and 2080s). Adjusted elevation rasters display the most probable range as determined by the Bayesian network, and the corresponding probability raster shows the likelihood of observing that outcome. Coastal response rasters show the probability of dynamic response; because the forecast is binary, the corresponding static response can be determined as the dynamic response probability shown subtracted from 1. Probability of 0.5 percent indicates total uncertainty in the CR prediction, meaning a static or dynamic response is deemed equally likely. Results span the coastal zone from elevations 10 m inland to –10 m offshore at a 30-m resolution matching that of the land-cover dataset.

Data Access

Predictions of the coastal landscape response to sea-level rise are available as part of this report (Lentz and others, 2015; http://dx.doi.org/10.5066/F73J3B0B). The data are assembled by year and correspond to the northeastern region of the United States as delineated by U.S. Department of the Interior Landscape Conservation Cooperatives (fig. 1; http://lccnetwork.org/find-an-lcc). The prediction data can also be accessed through the U.S. Geological Survey (USGS) Coastal Landscape Response to Sea-Level Rise Assessment project page (http://woodshole.er.usgs.gov/project-pages/coastal_response/). These predictions can be updated as new and improved input data become available for the region.

Metadata

Federal Geographic Data Committee-compliant metadata provided with each raster include detailed information on the model and probability predictions for use in interpreting the data contained within that file. The metadata, which vary by time step, include descriptions of the model (Bayesian network), the input data used, the time period over which the outputs were calculated, the spatial and temporal resolution of the outputs, and specific process steps and model parameters that would be necessary to recreate the results. Metadata also include any references, such as peer reviewed publications, reports, or Web sites that provide additional information on the data inputs, models and their parameterizations.

Data Quality Control

Quality-control checks are performed as part of model review, and errors are rectified before predictions are posted online. The following protocols are used to ensure data quality:

- Model input data are accessed directly from collaborators and published literature online;
- Data are extracted at the centroid of each land-cover cell from the highest resolution dataset available (where 1/9- and 1/3-arc-second elevation (NED) data are both available, 1/9-arc-second data are selected; where NED and CRM data are available, NED data are used);
- Data processing steps are documented and recorded;
- Model predictions (outputs) are validated against locations where coastal response characterization is well understood as available and appropriate;
- Output rasters (adjusted elevations, their probabilities, and coastal responses) are examined for outliers or other artifacts, and reviewed and interpreted by project scientists to verify that ranges,

patterns, and trends are reasonable and data and metadata formats are error free; if errors or inconsistencies are found, the model runs and geospatial conversions are reviewed and corrected as necessary; and

- The database manager reviews and verifies that metadata are complete and accurate and data format standards are met.

Data are continually assessed as they are used in analysis by the USGS and others. If errors or inconsistencies are discovered, the online data are updated and changes documented in the metadata.

References Cited

Arkema, K.K., Guannel, Greg, Verutes, Gregory, Wood, S.A., Guerry, Anne, Ruckelshaus, Mary, Kareiva, Peter, Lacayo, Martin, and Silver, J.M., 2013, Coastal habitats shield people and property from sea-level rise and storms: Nature Climate Change, v. 3, p. 913–918.

Bamber, J.L., and Aspinall, W.P., 2013, An expert judgment assessment of future sea-level rise from the ice sheets: Nature Climate Change, v. 3, no. 4, p. 424–427.

Bashari, H., Smith, C., and Bosch, O.J.H., 2009, Developing decision support tools for rangeland management by combining state and transition models and Bayesian belief networks: Agricultural Systems, v. 99, p. 23–34.

Bayes, Thomas, 1763, An essay towards solving a problem in the doctrine of chances: Philosophical Transactions of the Royal Society London, v. 53, p. 370–418. [Reprinted in Biometrika, 1958, v. 45, p. 296–315.]

Bender, M.A., Knutson, T.R., Tuleya, R.E., Sirutis, J.J., Vecchi, G.A., Garner, S.T., and Held, I.M., 2010, Modeled impact of anthropogenic warming on the frequency of intense Atlantic hurricanes: Science, v. 237, p. 454–458.

Brinson, M.M., Christian, R.R., and Blum, L.K., 1995, Multiple states in the sea-level induced transition from terrestrial forest to estuary: Estuaries, v. 18, no. 4, p. 648–659.

Cahoon, D.R., Reed, D.J., Kolker, A.S., Brinson, M.M., Stevenson, J.C., Riggs, Stanley, Christian, Robert, Reyes, Enrique, Voss, Christine, and Kunz, David, 2009, Coastal wetland sustainability, chap. 4 *of* Titus, J.G. [coordinating lead author], Anderson, K.E., Cahoon, D.R., Gesch, D.B., Gill, S.K., Gutierrez, B.T., Thieler, E.R., and Williams, S.J. [lead authors], Coastal sensitivity to sea-level rise—A focus on the mid-Atlantic region: Washington, D.C., U.S. Environmental Protection Agency, p. 57–72.

Calkin, D.E., Finney, M.A., Ager, A.A., Thompson, M.P., and Gebert, K.G., 2011, Progress towards and barriers to implementation of a risk framework for Federal wildland fire policy and decision making in the United States: Forest Policy and Economics, v. 13, p. 378–389.

Church, J.A., Clark, P.U., Cazenave, Anne, Gregory, J.M., Jevrejeva, Svetlana, Levermann, Anders, Merrifield, M.A., Milne, G.A., Nerem, R.S., Nunn, P.D., Payne, A.J., Pfeffer, W.T., Stammer, Detlef, and.Unnikrishnan, A.S., 2013, Sea-level change, chap. 13 *of* Stocker, T.F., Qin, Dahe, Plattner, G.-K., Tignor, M.M.B., Allen, S.K., Boschung, Judith, Nauels, Alexander, Xia, Yu, Bex, Vincent, and Midgley, P.M., eds., Climate change 2013—The physical science basis—Contribution of Working Group I to the Fifth Assessment Report of the Intergovernmental Panel on Climate Change: Cambridge, United Kingdom, Cambridge University Press, p. 1137–1216.

Clark, J.M., 1986, Coastal forest tree populations in a changing environment, southeastern Long Island, New York: Ecological Monographs, v. 56, no. 3, p. 259–277.

Craft, Christopher, Clough, Jonathan, Ehman, Jeff, Joye, Samantha, Park, Richard, Pennings, Steve, Guo, Hongyu, and Machmuller, Megan, 2009, Forecasting the effects of accelerated sea-level rise on tidal marsh ecosystem services: Frontiers in Ecology and the Environment, v. 7, no. 2, p. 73–78.

Field, C.B., Barros, Vicente, Stocker, T.F., Qin, Dahe, Dokken, D.J., Ebi, K.L., Mastrandrea, M.D., Mach, K.J., Plattner, G.-K., Allen, S.K., Tignor, Melinda, and Midgley, P.M., eds., 2012, Managing the risks of extreme events and disasters to advance climate change adaptation; special report of the Intergovernmental Panel on Climate Change: Cambridge, United Kingdom, Cambridge University Press, 582 p.

Fienen, M.N., Masterson, J.P., Plant, N.G., Gutierrez, B.T., and Thieler, E.R., 2013, Bridging groundwater models and decision support with a Bayesian network: Water Resources Research: v. 49, p. 6459–6473.

Fitzgerald, D.M., Fenster, M.S., Argow, B.A., and Buynevich, I.V., 2008, Coastal impacts due to sea-level rise: Annual Review of Earth and Planetary Sciences, v. 36, p. 601–647.

Fry, J.A., Xian, George, Jin, Suming, Dewitz, J.A., Homer, C.G., Yang, Limin, Barnes, C.A., Herold, N.D., and Wickham, J.D., 2011, Completion of the 2006 national land cover database for the conterminous United States: Photogrammetric Engineering and Remote Sensing, v. 77, no. 9, p. 858–864. [Also available at http://www.mrlc.gov/downloadfile2.php?file=September2011PERS.pdf.]

Gesch, D.B., 2007, The national elevation dataset, chap. 4 *of* Maune, D.F., ed., Digital elevation model technologies and applications—The DEM users manual (2d ed.): Bethesda, Md., American Society for Photogrammetry and Remote Sensing, p. 99–118.

Gesch, D.B., 2009, Analysis of lidar elevation data for improved identification and delineation of lands vulnerable to sea-level rise: Journal of Coastal Research, special issue 53, p. 49–58.

Gieder, K.D., Karpanty, S.M., Fraser, J.D, Catlin, D.H., Gutierrez, B.T., Plant, N.G., Turecek, A.M., and Thieler, E.R., 2014, A Bayesian network approach to predicting nest presence of the federally-threatened piping plover (*Charadrius melodus*) using barrier island features: Ecological Modelling, v. 276, p. 38–50.

Gutierrez, B.T., Plant, N.G., and Thieler, E.R., 2011, A Bayesian network to predict the coastal vulnerability to sea-level rise: Journal of Geophysical Research, v. 116, p. 1–15.

Gutierrez, B.T., Williams, S.J., and Thieler, R.T., 2009, Ocean coasts, *in* Titus, J.G. [coordinating lead author], Anderson, K.E., Cahoon, D.R., Gesch, D.B., Gill, S.K., Gutierrez, B.T., Thieler, E.R., and Williams, S.J. [lead authors], Coastal sensitivity to sea-level rise—A focus on the mid-Atlantic region: Washington, D.C., U.S. Environmental Protection Agency, p. 43–56.

Hapke, C.J. and Plant, N.P., 2011, Predicting coastal cliff erosion using a Bayesian probabilistic model: Marine Geology, v. 278, nos. 1–4, p. 140–1499.

Hartmann, D.L., Klein Tank, A.M.G., Rusticucci, Matilde, Alexander, L.V., Brönnimann, Stefan, Charabi, Y.A.-R., Dentener, F.J., Dlugokencky, E.J., Easterling, D.R., Kaplan, Alexey, Soden, B.J., Thorne, P.W., Wild, Martin, and Zhai, Panmao, 2013, Observations—Atmosphere and surface, chap. 2 *of* Stocker, T.F., Qin, Dahe, Plattner, G.-K., Tignor, M.M.B., Allen, S.K., Boschung, Judith, Nauels, Alexander, Xia, Yu, Bex, Vincent, and Midgley, P.M., eds., Climate change 2013—The physical science basis—Contribution of Working Group I to the Fifth Assessment Report of the Intergovernmental Panel on Climate Change: Cambridge, United Kingdom, Cambridge University Press, p. 159–254.

Horton, Radley, Yohe, Gary, Easterling, William, Kates, Robert, Ruth, Matthias, Sussman, Edna, Whelchel, Adam, Wolfe, David, and Lipschultz, Fredric, 2014, Northeast, chap. 16 *of* Melillo, J.M., Richmond, T.C., and Yohe, G.W., eds., Climate change impacts in the United States—The third national climate assessment: Washington, D.C., U.S. Global Change Research Program, p. 371–395.

Jin, Suming, Yang, Limin, Danielson, Patrick, Homer, Collin, Fry, Joyce, and Xian, George, 2013, A comprehensive change detection method for updating the national land cover database to circa 2011: Remote Sensing of the Environment, v. 132, p. 159–175.

Karl, T.R., Melillo, J.M., and Peterson, T.C., eds., 2009, Global climate change impacts in the United States: Cambridge, United Kingdom, Cambridge University Press, 189 p.
Kirwan, M.L., Guntenspergen, G.R., D'Alpaos, Andrea, Morris, J.T., Mudd, S.M., and Temmerman, Stijn, 2010, Limits on the adaptability of coastal marshes to rising sea-level: Geophysical Research Letters, v. 37, no. 23, 5 p.
Kirwan, M.L., Kirwan, J.L., and Copenheaver, C.A., 2007, Dynamics of an estuarine forest and its response to rising sea-level: Journal of Coastal Research, v. 23, no. 2, p. 457–463.
Kirwan, M.L., and Megonigal, J.P., 2013, Tidal wetland stability in the face of human impacts and sea-level rise: Nature, v. 504, p. 53–60.
Lentz, E.E., Stippa, S.R., Thieler, E.R., Plant, N.G., Gesch, D.B., and Horton, R.M., 2015, Coastal landscape response to sea-level rise assessment for the northeastern United States (ver. 2.0, December 2015): U.S. Geological Survey data release, http://dx.doi.org/10.5066/F73J3B0B.
Marcot, B.G., Thompson, M.P., Runge, M.C., Thompson, F.R., McNulty, Steven, Cleaves, David, Tomosy, Monica, Fisher, L.A., and Bliss, Andrew, 2012, Recent advances in applying decision science to managing national forests: Forest Ecology and Management, v. 285, p. 123–132.
Marcy, Doug, Brooks, William, Draganov, Kyle, Hadley, Brian, Haynes, C., Herold, Nate, McCombs, John, Pendleton, Matt, Ryan, Sean, Schmid, Keil, Sutherland, Mike, and Waters, Kirk, 2011, New mapping tool and techniques for visualizing sea-level rise and coastal flooding impacts, *in* Wallendorf, Louise, Jones, Chris, Ewing, Lesley, and Battalio, Bob, eds., Solutions to Coastal Disasters 2011, Anchorage, Alaska, June 25–29, 2011, proceedings: Reston, Va., American Society of Civil Engineers, p. 474–490.
Martin, Julien, Fackler, P.L., Nichols, J.D., Lubow, B.C., Eaton, M.J., Runge, M.C., Stith, B.M., and Langtimm, C.A., 2011, Structured decision making as a proactive approach to dealing with sea-level rise in Florida: Climatic Change, v. 107, p. 185–202.
Marzion, B., Jarosch, A.H., and Hofer, M., 2012, Past and future sea-level change from the surface mass balance of glaciers: The Cryosphere, v. 6, no. 6, p. 1295–1322.
Masterson, J.P., Fienen, M.N., Thieler, E.R., Gesch, D.B., Gutierrez, B.T., and Plant, N.G., 2013, Effects of sea-level rise on barrier island groundwater system dynamics—Ecohydrological implications: Ecohydrolology, v. 7, no. 3., p. 1064–1071.
McNamara, D.E., and Keeler, Andrew, 2013, A coupled physical and economic model of the response of coastal real estate to climate risk: Nature Climate Change, v. 3, p. 559–562.
McNamara, D.E., Murray, A.B., and Smith, M.D., 2011, Coastal sustainability depends on how economic and coastline response to climate change affect each other: Geophysical Research Letters, v. 38, no. 7, 5 p.
McNamara, D.E., and Werner, B.T., 2008, Coupled barrier island-resort model—1. Emergent instabilities induced by strong human-landscape interactions: Journal of Geophysical Research, v., 113, F01016, 10 p.
Morris, J.T., Sundareshwar, P.V., Nietch, C.T., Kjerfve, Björn, and Cahoon, D.R., 2002, Responses of coastal wetlands to rising sea level: Ecology, v. 83, p. 2869–2877.
Moser, S.C., Davidson, M.A., Kirshen, Paul, Mulvaney, Peter, Murley, J.F., Neumann, J.E., Petes, Laura, and Reed, Denise, 2014, Coastal zone development and ecosystems, chap. 25 *of* Melillo, J.M., Richmond, T.C., and Yohe, G.W., eds., Climate change impacts in the United States—The third National Climate Assessment: Washington, D.C., U.S. Global Change Research Program, p. 579–618.
National Ocean Service, 2012, VDatum manual for development and support of NOAA's vertical datum transformation tool, VDatum (ver. 1.01): National Oceanic and Atmospheric Administration and National Geodetic Survey, 119 p. [Also available at http://vdatum.noaa.gov/docs/publication.html.]

National Oceanic and Atmospheric Administration National Geophysical Data Center, 2014, U.S. coastal relief model: National Oceanic and Atmospheric Administration National Geophysical Data Center Web page, accessed June 2014 at http://www.ngdc.noaa.gov/mgg/coastal/crm.html.
National Research Council, 2009, Science and decisions—Advancing risk assessment: Washington, D.C., The National Academies Press, 478 p.
Niederoda, A.W., Swift, D.J.P., Hopkins, T.S., and Meanima, C.-M., 1984, Shoreface morphodynamics on wave-dominated coasts: Marine Geology, v. 60, p. 331–354.
Ogden, A.E., and Innes, J.L., 2009, Application of structured decision making to an assessment of climate change vulnerabilities and adaptation options for sustainable forest management: Ecology and Society: v. 14, no. 1, [article 11], accessed November 3, 2014, at http://www.ecologyandsociety.org/vol14/iss1/art11/.
Orth, R.J., Carruthers, T.J.B., Dennison, W.C., Duarte, C.M., Fourqurean, J.W., Heck, K.L., Jr., Hughes, A.R., Kendrick, G.A., Kenworthy, W.J., Olyarnik, Suzanne, Short, F.T., Waycott, Michelle, and Williams, S.L., 2006, A global crisis for seagrass ecosystems: Bioscience, v. 56, no. 12, p. 987–996.
Plant, N.G., Flocks, James, Stockdon, H.F., Long, J.W., Guy, Kristy, Thompson, D.M., Cormier, J.M., Smith, C.G., Miselis, J.L., and Dalayander, P.S., 2014, Predictions of barrier island berm evolution in a time-varying storm climatology: Journal of Geophysical Research, v. 119, no. 2, p. 300–316.
Plant, N.G., and Holland, K.T., 2011, Prediction and assimilation of surf-zone processes using a Bayesian network—Part I—Forward models: Coastal Engineering, v. 58, no. 1, p. 119–130.
Plant, N.G., and Stockdon, H.F., 2012, Probabilistic prediction of barrier-island response to hurricanes: Journal of Geophysical Research, v. 117, F03015, 17 p.
Radić, Valentina, Bliss, Andrew, Beedlow, C.D., Hock, Regine, Miles, Evan, and Cogley, J.G., 2013, Regional and global projections of twenty-first century glacier mass changes in response to climate scenarios from global climate models: Climate Dynamics, v. 42, nos. 1–2, p. 37–58.
Robichaud, A., and Begin, Y., 1997, The effects of storms and sea-level rise on a coastal forest margin in New Brunswick, eastern Canada: Journal of Coastal Research, v. 13, no. 2, p. 429–439.
Rotzol, Kolja, and Fletcher, C.J., 2013, Assessment of groundwater inundation as a consequence of sea-level rise: Nature Climate Change, v. 3, p. 477–481. Runge, M.C., Converse, S.J., and Lyons, J.E., 2011, Which uncertainty?—Using expert elicitation and expected value of information to design an adaptive program: Biological Conservation, v. 144, p. 1214–1223.
Seavey, J.R., Gilmer, Ben, and McGarigal, K.M., 2011, Effect of sea-level rise on piping plover (*Charadrius melodus*) breeding habitat: Biological Conservation, v. 144, p. 393–401.
Sella, G.F., Stein, Seth, Dixon, T.H., Craymer, Michael, James, T.S., Mazzotti, Stephane, and Dokka, R.K., 2007, Observation of glacial isostatic adjustment in "stable" North America with GPS: Geophysical Research Letters, v. 34, L02306, 6 p.
Swift, D.J.P., Niederoda, A.W., Vincent, C.E., and Hopkins, T.S., 1985, Barrier island evolution, middle Atlantic shelf, U.S.A.; Part I—Shoreface dynamics: Marine Geology, v. 63, p. 331–361.
Taylor, K.E., Stouffer, R.J., and Meehl, G.A., 2012, An overview of CMIP5 and the experiment design: Bulletin of the American Meteorological Society, v. 93, no. 4, p. 485–498.
Thieler, E.R., and Hammar-Klose, E.S., 1999, National assessment of coastal vulnerability to future sea-level rise—Preliminary results for the U.S. Atlantic coast: U.S. Geological Survey Open-File Report 99–593, 1 sheet. [Also available at http://pubs.usgs.gov/of/of99-593/.]
U.S. Army Corps of Engineers, 2013, Coastal risk reduction and resilience—Using the full array of measures: U.S Army Corps of Engineers Civil Works Technical Series 2013–3, 11 p., 1 appendix.

U.S. Geological Survey, 2014, National elevation dataset: U.S. Geological Survey database, accessed August 30, 2012, at http://ned.usgs.gov/.
Weiss, J.L., Overpeck, J.T., and Strauss, Ben, 2011, Implications of recent sea-level rise science for Low-elevation areas in coastal cities of the conterminous U.S.A.: Climatic Change, v. 105, p. 635–645.
Williams, Kimberlyn, Ewel, K.C., Stumpf, R.P., Putz, F.E., and Workman, T.W., 1999, Sea-level rise and coastal forest retreat on the west coast of Florida, USA: Ecology, v. 80, no. 6, p. 2045–2063.
Wong, P.P., Losada, I.J., Gattuso, J.P., Hinkel, Jochen, Khattabi, Abdellatif, McInnes, K.L., Saito, Yoshiki, and Sallenger, Asbury, 2014, Coastal systems and low-lying areas, chap. 5 *of* Field, C.B., Barros, V.R., Dokken, D.J., Mach, K.J., Mastrandrea, M.D., Bilir, T.E., Chatterjee, Monalisa, Ebi, K.L., Estrada, Y.O., Genova, R.C., Girma, Betelhem, Kissel, E.S., Levy, A.N., MacCracken, Sandy, Mastrandrea, P.R.,, and White, L.L., eds., Climate change 2014—Impacts, adaptation, and vulnerability—Part A—Global and sectoral aspects—Contribution of Working Group II to the Fifth Assessment Report of the Intergovernmental Panel on Climate Change: Cambridge, United Kingdom, Cambridge University Press, p. 361–409.
Wright, L.D.; Boon, J.D.; Kim, S.C., and List, J.H., 1991, Modes of cross-shore sediment transport on the shoreface of the middle Atlantic bight: Marine Geology, v. 96, p. 19–51.
Wright, L.D., Xu, J.P., and Madsen, O.S., 1994, Across-shelf benthic transports on the inner shelf of the Middle Atlantic Bight during the “Halloween storm” of 1991: Marine Geology, v. 118, nos. 1–2, p. 61–77.
Zervas, Chris, Gill, Stephen, and Sweet, William, 2013, Estimating vertical land motion from long-term tide gauge records: National Oceanic and Atmospheric Administration Technical Report NOS CO–OPS 065, 30 p.

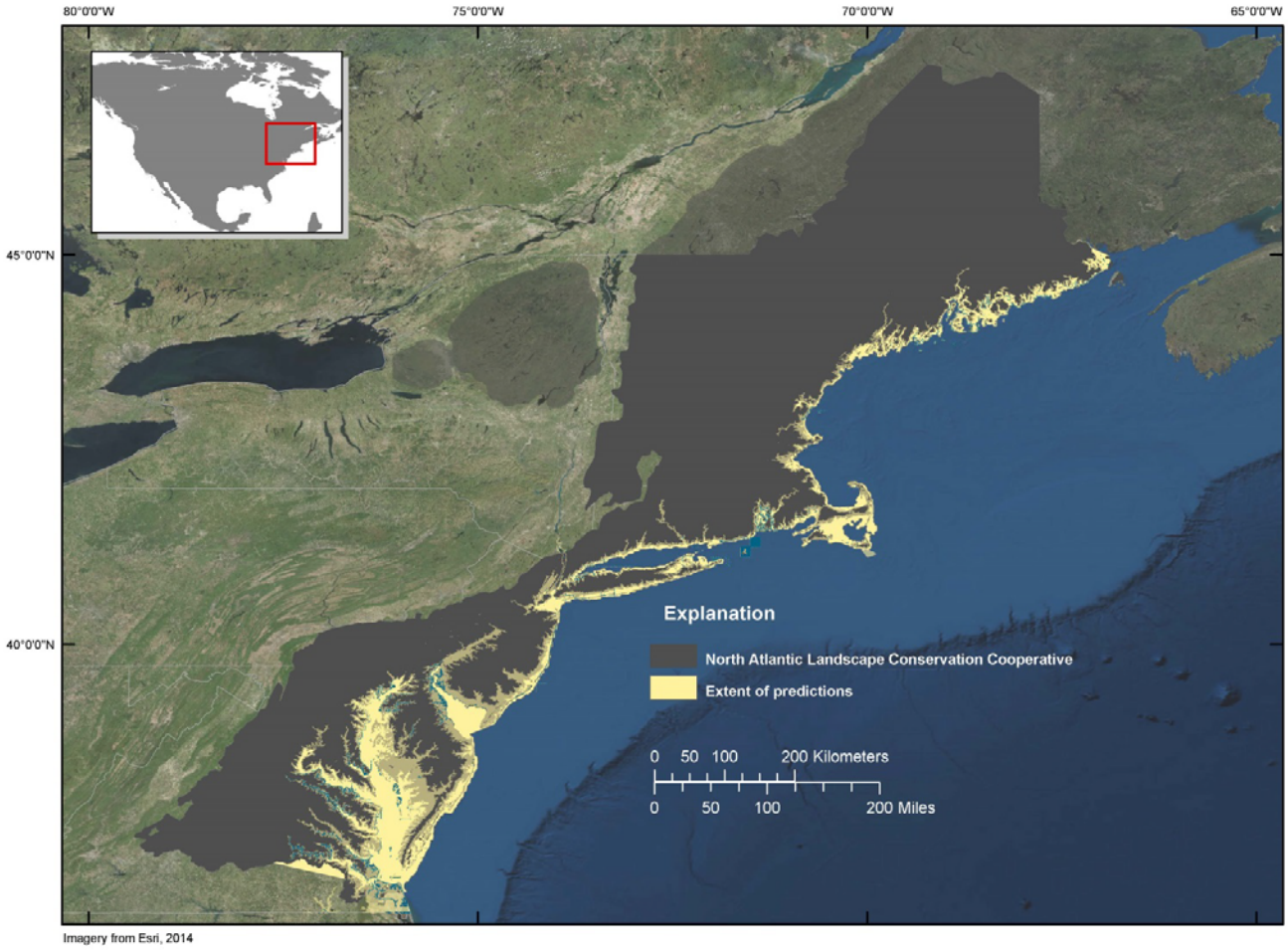

Figure 1. Map showing coastal extent of regional predictions from Maine to Virginia (yellow) within the boundary of the North Atlantic Landscape Conservation Cooperative (gray). North Atlantic Landscape Conservation Cooperative boundary is from U.S. Fish and Wildlife Service (2012).

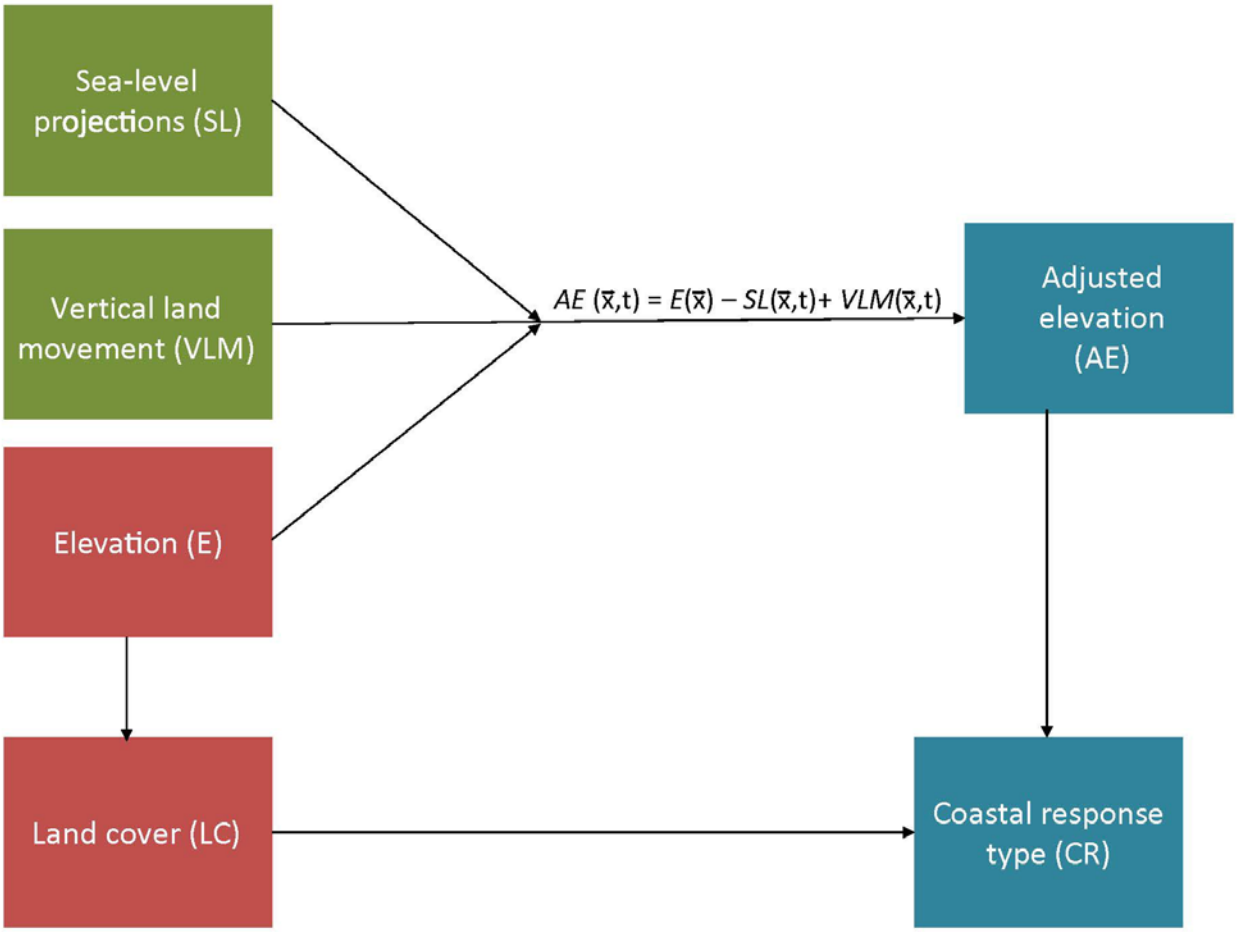

Figure 2. Conceptual diagram showing the structure of the Bayesian network. Sea-level projections (*SL*) and vertical land movement (*VLM*) are driving forces (green boxes), elevation (*E*) and land cover (*LC*) are boundary conditions (red boxes), and adjusted elevation (*AE*) and coastal response type (*CR*) are the sea-level-rise response variables (blue boxes). The equation shown relates *SL*, *VLM*, and *E* to produce *AE* predictions, whereas *AE* predictions and *LC* (table 1) are related through expert knowledge (ref. table 2) to produce *CR* predictions.

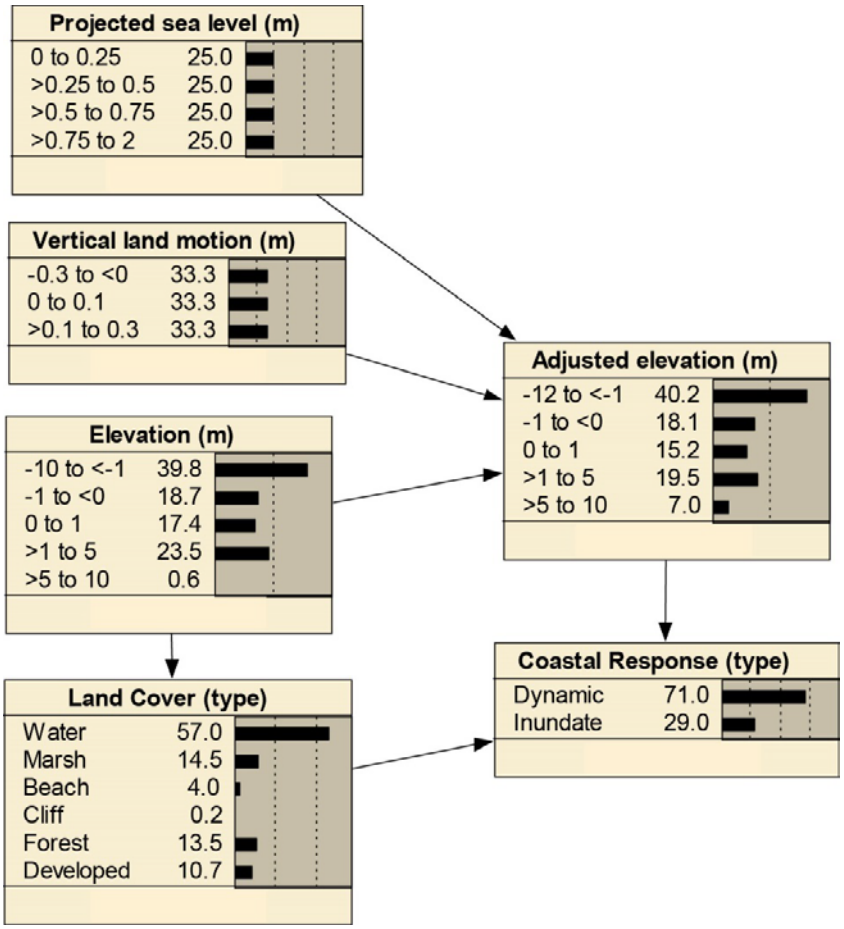

Figure 3. Diagram showing Bayesian network configuration, including inputs (left) and outputs (right). Horizontal bars shown in the boxes represent prior distributions (probability of occurrence) for each parameter, with uniform distributions assigned to projected sea-level and vertical land motion parameters to provide an equal likelihood of occurrence among them until a time step is specified. Correlations among nodes are shown by the arrows between them. Probabilities may not add up to exactly 100 percent due to independent rounding. m, meters.

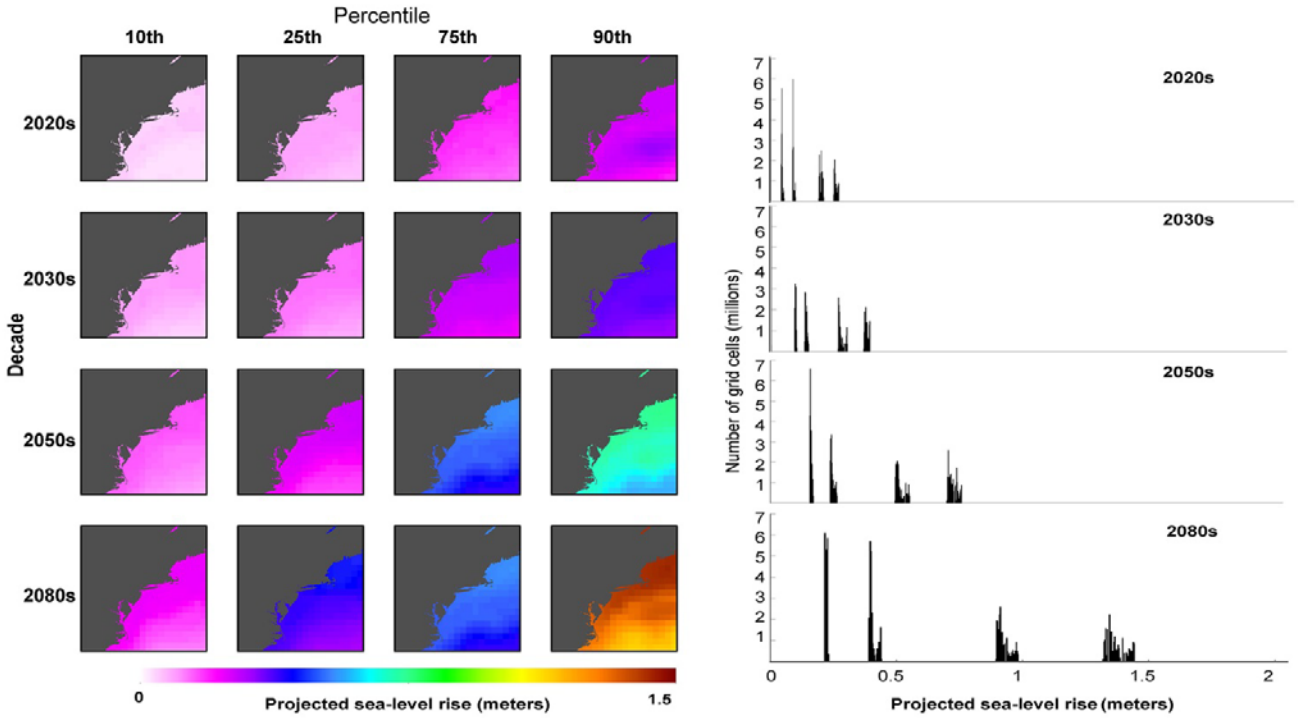

Figure 4. Projected sea-level rise in decadal averages; left side shows gridded (1- by 1-degree resolution) outputs in the four percentile ranges, and right side shows the number of grid cells in each percentile range within the study area.

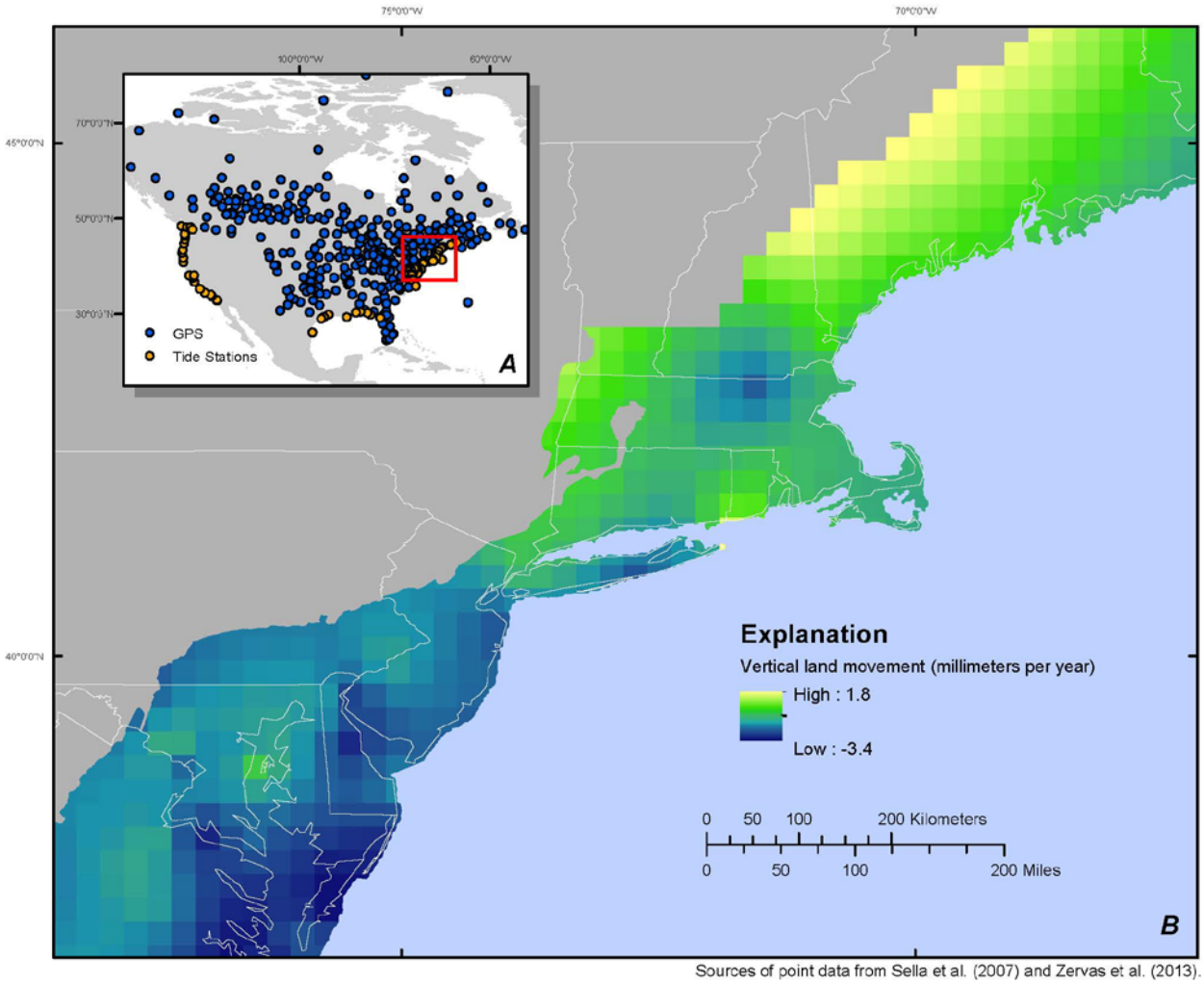

Figure 5. Maps showing vertical land movement rates at *A*, Global Positioning System (GPS) and tide station point locations and *B*, as an interpolated surface across the North Atlantic Landscape Conservation Cooperative region from which model inputs were extracted at land-cover point locations.

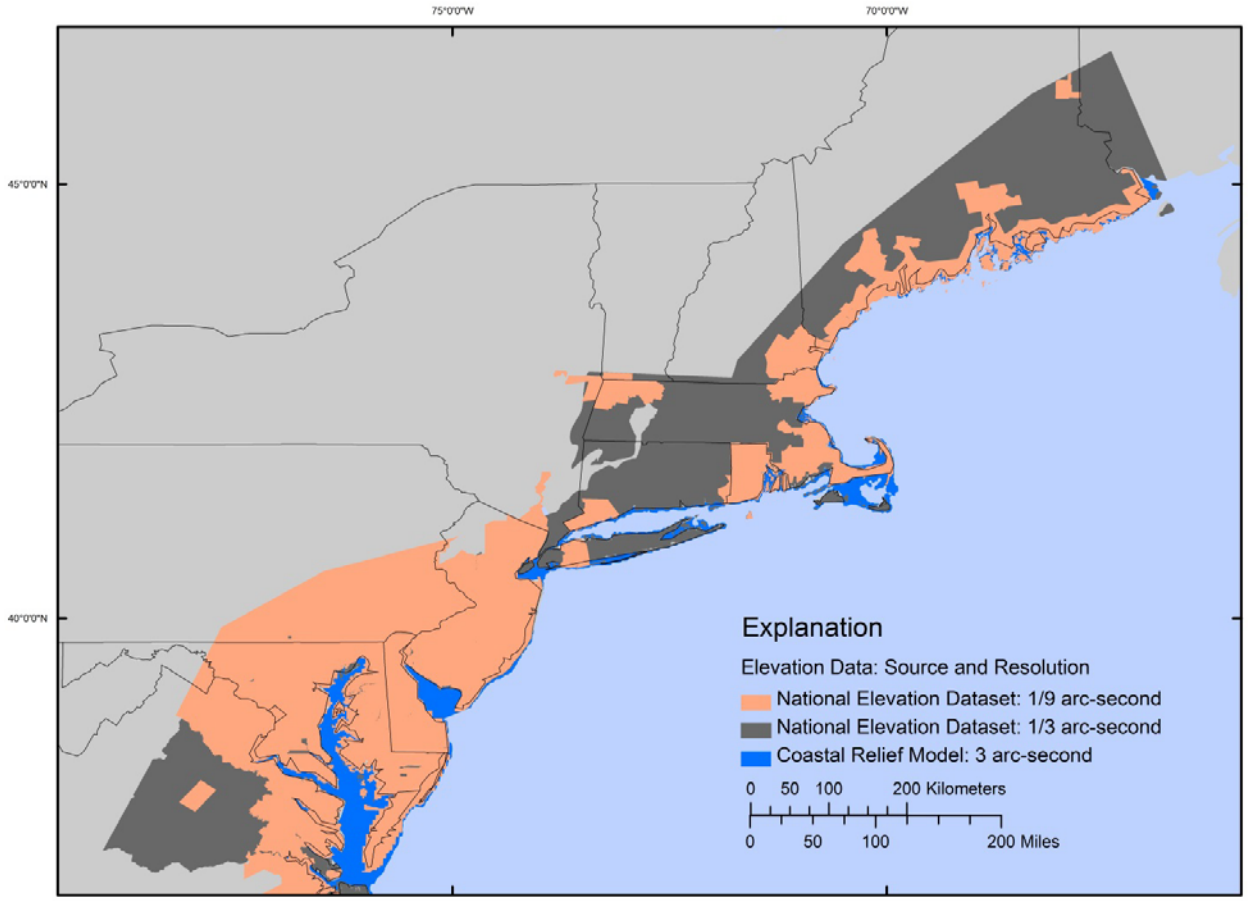

Figure 6. Map showing sources and coverage of land elevation data (topography and bathymetry) for the North Atlantic Landscape Conservation Cooperative region (orange and gray); supplemental bathymetric data to the -10-m contour offshore are shown in blue. Data are from U.S. Geological Survey (2014) and National Oceanic and Atmospheric Administration National Geophysical Data Center (2014).

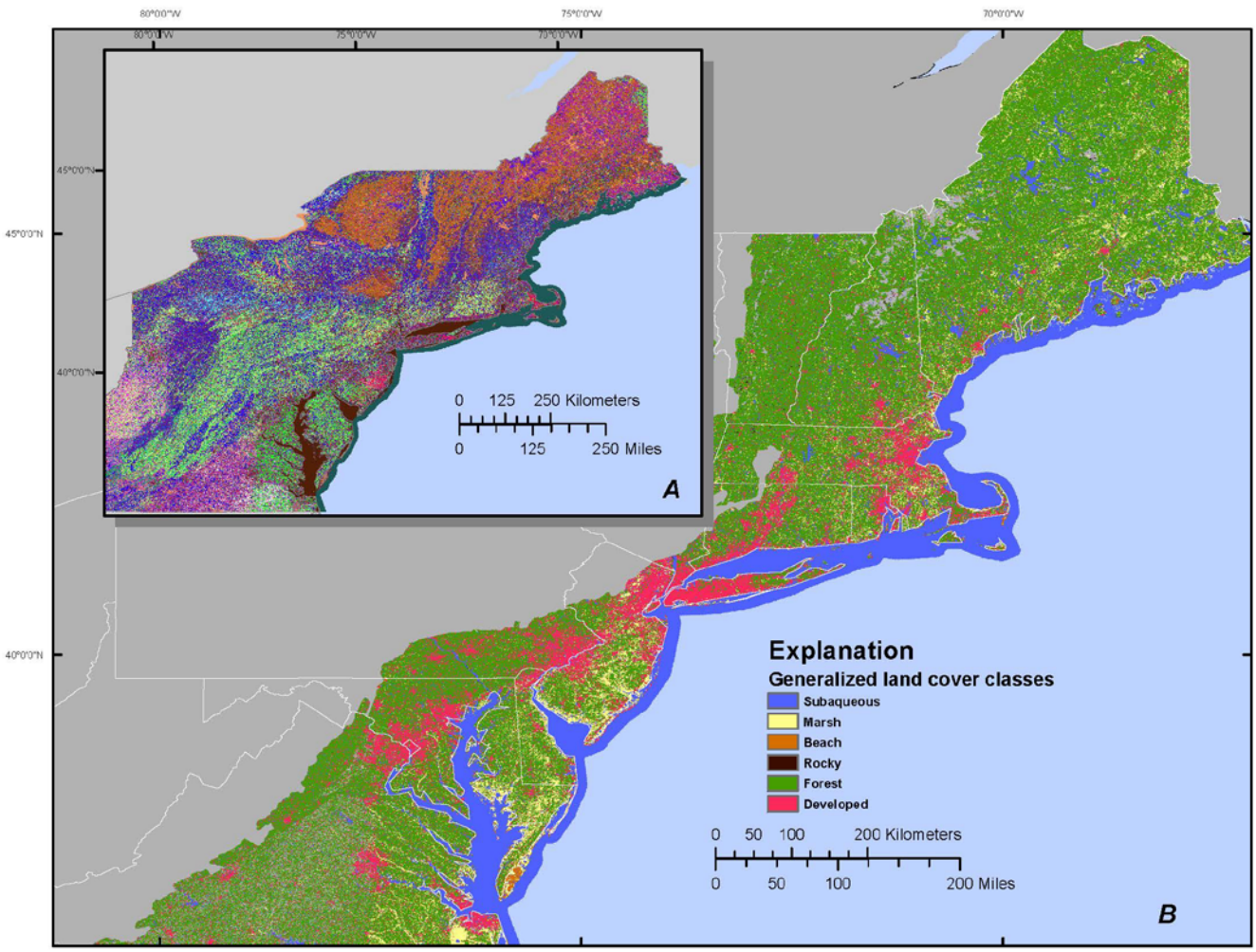

Figure 7. Maps showing geospatial distribution of the land-cover data *A*, as shown in Ecological Systems Map (ESM) Plus (ESMplus) and *B*, as generalized to the six land-cover categories used in this study. ESMplus digital data from the Designing Sustainable Landscapes Project, University of Massachusetts (2014).

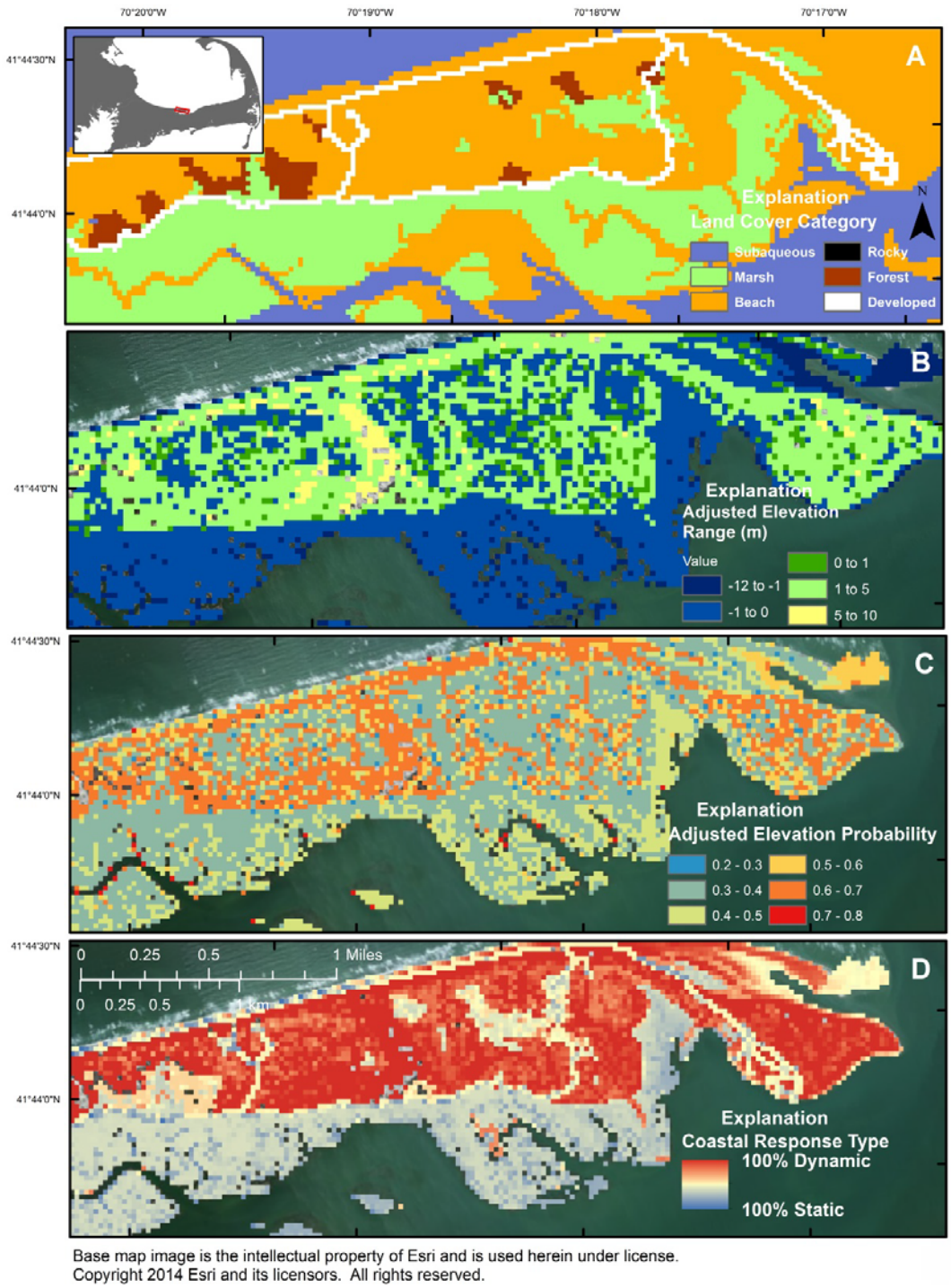

Figure 8. Example 2050 prediction results for Sandy Neck in Barnstable, Massachusetts, showing *A*, generalized land-cover information, *B*, adjusted elevation (AE) ranges with respect to mean high water, *C*, the prediction probability or likelihood of observing the AE prediction, and *D*, the likelihood that the coastal response is dynamic or static.

For more information concerning this report, contact:
Director, Woods Hole Coastal and Marine
Science Center
U.S. Geological Survey
384 Woods Hole Road
Quissett Campus
Woods Hole, MA 02543-1598
WHSC_science_director@usgs.gov
508-548-8700 or 508-457-2200
or visit our Web site at:
http://woodshole.er.usgs.gov/

Publishing support by:
The Pembroke Publishing Service Center.

ISSN 2331-1258 (online)
http://dx.doi.org/10.3133/ofr20141252